



FLEXURAL BEHAVIOR OF UNDER-REINFORCED STEEL FIBER CONCRETE (R/SFRC) BEAMS

Daniel C. T. Cardoso⁽¹⁾, **Gabriel B. S. Pereira**⁽¹⁾, **Julio J. S. Holtz Filho**⁽¹⁾, **Flávio A. Silva**⁽¹⁾, **Eric V. Pereira**⁽¹⁾

(1) Department of Civil and Environmental Engineering, Pontifícia Universidade Católica do Rio de Janeiro, Brazil

<https://doi.org/10.21452/bccm4.2018.02.30>

Abstract

This paper reports the findings of an experimental program aiming to investigate the influence of steel fibers in the flexural behavior of under-reinforced reinforced concrete beams (S/SFRC). Hooked end steel fibers with aspect ratios of 48 or 60 were used to produce matrices with fiber content ranging from 0 to 2%, in volume. A full mechanical characterization was carried for each matrix studied, as well as for the reinforcing steel used. Reduced scale beams with reinforcing ratios of 0.28, 0.44 and 0.70% were instrumented with strain gages and displacement transducers. Digital image correlation (DIC) was also used to monitor strain field and crack formation and growth throughout the constant moment region during loading. Experimental load-deflection and moment-curvature relationships are reported, showing gains of capacity ranging from 21 to 109% with respect to conventional reinforced concrete (RC) beams. Increases in cracked stiffness were also observed and all beams presented ductility within desired limits. The results obtained using analytical models are compared to the experimental results and excellent agreement achieved shows that models can be successfully adopted to predict the actual behavior of R/SFRC beams in flexure. Finally, crack formation and growth are reported, showing that the use of steel fibers leads to a pattern characterized by multiple small cracks and a critical wider crack, but with opening much smaller than that obtained for RC.

1. INTRODUCTION

Introduced during the 1960's, fibrous concrete – or fiber-reinforced concrete (FRC) – is defined as a concrete containing dispersed randomly oriented fibers and its advantages over plain concrete include post-crack tensile residual strength and enhanced toughness. FRC has gained acceptance among civil engineers and has been widely adopted in applications such as slabs on ground, precast pipes and façade panels, retaining walls and tunnel linings as an alternative to conventional reinforced concrete [1, 2]. On the other hand, the use of conventional flexural reinforcement combined with FRC in load-carrying members has been very limited [3, 4], despite the advantages with respect to conventional RC, including: i)

improve in shear strength, leading to the possibility to fully or partially substitute stirrups by fibers; ii) increased flexural stiffness and strength; and iii) improvement of adherence between concrete and steel, leading to multiple crack formation and a better crack width control at serviceability limit states [1, 5].

The flexural behavior of reinforced steel fiber concrete (R/SFRC) beams has been investigated by several authors, but Henager and Doherty [6] were the first to propose an analytical approach to the strength of R/SFRC beams. In the method, the bending strength is determined assuming the rectangular stress blocks for concrete in tension and compression zones. In their study, Henager and Doherty [6] observed an increase up to 25% in strength with respect to conventional RC and good agreement was achieved between proposed approach and experimental results for beams containing 1.22 to 1.51% of straight fibers in volume (aspect ratios $l_f/d_f = 38$ and 57) and low yield strength steel. The method was also successfully used by other authors in comparison with experiments considering different material properties and cross-section configurations [7-10], showing that, apparently, the design strategy can be adopted regardless reinforcing steel, fiber volume fraction, type of fiber and concrete compressive strength. This approach is currently recommended by fib Model Code 2010 [11] for the design of S/SFRC beams. A different approach to strength was recently proposed by Van Zijl and Mbewe [12], assuming that failure may occur before concrete reaches the strain corresponding to the stress peak in compression. Linear and non-linear stress distributions were considered in the study and a parametric study was carried on. To validate the method, five beams having 1.0 and 1.5% by volume of hooked end fibers ($l_f/d_f = 60$) and high tensile yield strength bars were tested in bending. The authors concluded that Henager and Doherty's approach underpredicted the experimental results, while better agreement was achieved for their proposed approach. It was also acknowledged that strain-hardening of steel bars may increase significantly the bending capacity.

To investigate the influence of reinforcing ratio in failure modes, capacity and ductility of R/SFRC beams, Mertol *et al.* [13] tested 20 beams having $V_f = 0$ or 1% (hooked end fibers with $l_f/d_f = 60$) and ρ_s ranging from 0.2 to 2.5%. Classification of sections in over- and under-reinforced groups were made based on the balanced ratio calculated (1.6%) for conventional RC. Trends in behavior were reported by the authors, such as the slight increase in capacity and in stiffness for R/SFRC specimens and the significant improve in toughness for specimens having $\rho_s > 0.4\%$. Results from load-deflection curves were finally compared with predictions made using different assumed stress-strain models for concrete in compression. From tables reported by authors, a large deviation can be observed between theory and experiments, which can be explained by the following reasons: i) a full material characterization has not been carried out by authors; ii) the conversion of moment-curvature relationships obtained from theoretical models in load-deflection response used in the work and proposed by other authors [14, 15] is not straightforward due to the contribution of uncracked concrete in tension zone (tension-stiffening effect).

In the present work, the results from an experimental program carried out on R/SFRC beams subject to 4-point bending are reported. For a comprehensive study, the testing program included the use hooked end steel fibers with $l_f/d_f = 45$ and 80 , with contents in volume ranging from 0 to 2% and different reinforcing ratios. To allow a better comparison with theory, a full material characterization was conducted to obtain representative stress-strain models and curvatures and neutral axis depths were measured in the constant moment region using digital image correlation (DIC). From the validated models, it is possible to clearly determine the contributions of conventional reinforcement and fibers to the behavior. Crack growth and patterns are also reported.

2. EXPERIMENTAL PROGRAM

The experimental program consisted in flexural tests of R/SFRC beams having different fiber types and contents and reinforcing ratios. A full material characterization was also performed.

2.1 Materials

The materials used in the production of the concrete matrix used in the self-compacting SFRC were: natural river sand, gravel, high early strength cement, fly ash, active silica, Silica 325, hook-ended steel fiber and superplasticizer. Two different types Dramix® fiber were considered in the study: 45/30 and 80/60 (“aspect ratio/fiber length”). Table 1 shows the mix proportions adopted in the study.

Table 1: Concrete mixture proportions per m³.

Materials	Quantity (kg)
Cement (Type III)	360
Gravel (9.5 mm)	494
Natural sand #.85	830
Natural sand #.15	100
Silica 325	70
Fly Ash	168
Active silica	45
Superplasticizer	45
Water	150
Steel fiber	0, 39.3, 78.5 and 157*

* respectively for 0, 0.5, 1 and 2% of fiber content in volume

2.2 Mechanical Characterization

To obtain the relevant mechanical properties of materials used in the study, the following tests were carried out: cylinder compression and direct tension of SFRC matrix; and tensile test for reinforcing steel. At least three specimens for each matrix and bar diameter considered in the study were tested (except for 6.3 mm rebar, not tested). In Figure 1, representative stress-strain relationships are presented. It is important to note that, for the tensile test, term ‘strain’ refers to the bar elongation divided by the gage length. Properties obtained for concrete matrix and reinforcing steel are summarized in Tables 2 and 3, respectively.

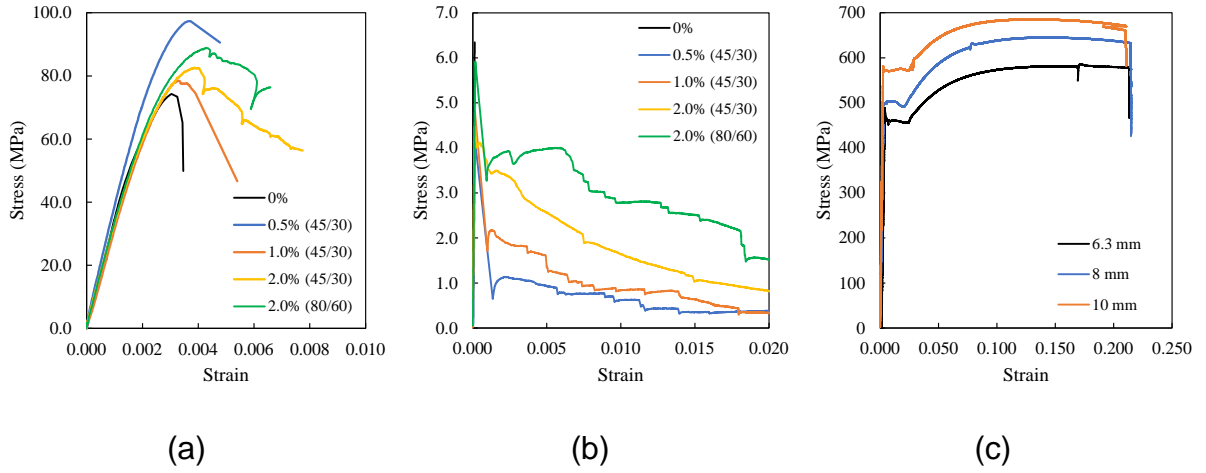


Figure 1 : Representative stress-strain relationships: a) cylinder compression; b) direct tension of matrix; and c) rebar tension.

Table 2: Summary of mechanical properties for concrete matrix.

Property	V_f (%)				
	0	0.5	1.0	2.0(45/30)	2.0 (80/60)
Compressive strength f_c' (MPa)	76.3 ± 1.8	95.2 ± 1.4	80.2 ± 2.5	81.3 ± 2.3	84.9 ± 3.8
Compressive strain at peak ε_{c0} (‰)	3.03 ± 0.01	3.65 ± 0.11	3.29 ± 0.52	3.30 ± 0.82	3.99 ± 0.36
Tensile strength f_{ct} (MPa)	6.04 ± 0.89	4.96 ± 0.69	5.12 ± 0.23	4.54 ± 0.31	5.15 ± 0.55
Tensile strain at peak ε_{t0} (‰)	0.13 ± 0.01	0.16 ± 0.01	0.16 ± 0.02	0.13 ± 0.02	0.15 ± 0.02
Tensile modulus E_c (GPa)	46.5	31.0	32.0	34.9	34.3
Tensile stress for 'strain' 10‰ $f_{ctr,10}$ (MPa)	-	0.67 ± 0.39	1.13 ± 0.25	1.75 ± 0.46	2.70 ± 0.46
Tensile stress for 'strain' 5‰ $f_{ctr,5}$ (MPa)	-	1.27 ± 0.50	1.83 ± 0.35	2.53 ± 0.49	3.68 ± 0.37

Table 3: Summary of mechanical properties for reinforcing steel.

	Rebar diameter ϕ (mm)	
	8	10
Yielding strength f_y (MPa)	497 ± 18	553 ± 18
Strain at yielding ε_y (‰)	2.28 ± 0.13	2.75 ± 0.20
Elastic modulus E_s (GPa)	218 ± 8	203 ± 20

2.3 Beam Tests

To study the behavior of beams reinforced with conventional steel and discrete fibers, nine 15x15x120 cm beams with 2-cm cover were fabricated in laboratory and tested in four-point bending over a span of 110 cm with a constant moment region length of 37 cm. Testing

matrix is presented in Table 3 and it can be noted that three control specimens without fibers and with different reinforcing ratios were produced to allow comparison with results for R/SFRC beams. To induce first crack at midspan, a triangular-shaped notch 1.5-cm-wide x 1.0-cm-tall was introduced at the middle of the bottom face of each specimen. To avoid shear rupture, 5-mm-diameter stirrups were adopted along shear spans. To measure crack kinematics and to obtain curvature at cracked section with load, 2D digital image correlation analysis (DIC-2D) was carried out to obtain the displacement field at the constant moment region. Data were calculated from a sequence of high resolution images obtained during the test and compared with a reference image. Alternatively, to monitor the strains during loading, strain gages were used in three different positions of each rebar and other two positioned at the beam top face. Beam deflections at midspan were measured with a displacement transducer. Tests were conducted up to failure with displacement control at a rate of 2 mm/min using an MTS actuator with 500 kN capacity. Figure 2 shows an overview of test setup.

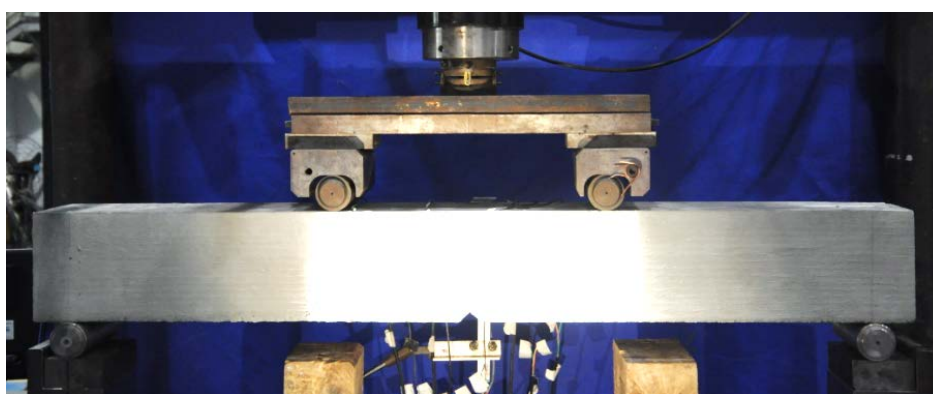


Figure 2: Overview of setup for 4-point bending tests.

Table 3: Beam testing matrix.

Specimen	V_f (%)	Fiber type	Bar diameter (mm)	Number of bars	Reinforcing ratio (%)
B1-0-6	0	HE 45/30	6.3	2	0.28
B2-0-8	0	HE 45/30	8	2	0.44
B3-0-10	0	HE 45/30	10	2	0.70
B4-0.5/S-10	0.5	HE 45/30	10	2	0.70
B5-1/S-10	1	HE 45/30	10	2	0.70
B6-2/S-6	2	HE 45/30	6.3	2	0.28
B7-2/S-8	2	HE 45/30	8	2	0.44
B8-2/S-10	2	HE 45/30	10	2	0.70
B9-2/L-10	2	HE 80/60	10	2	0.70

3. DISCUSSION OF RESULTS

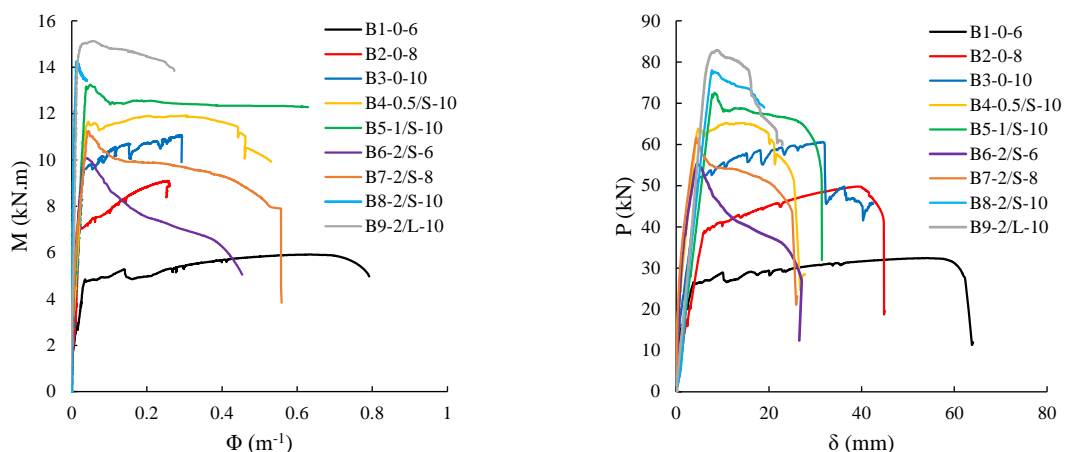
All tested beams exhibited significant crack opening prior to failure and, based on strain gage readings, yielding of reinforcing steel occurred in all cases. Typical failure modes

observed for RC and R/SFRC beams are presented in Figure 3. For RC beams, wide cracks regularly spaced formed along the constant moment region and failure mode was characterized by excessive deformation of reinforcement. For R/SFRC beams, one or two wider cracks could be clearly identified and failure was governed by fiber pull-out followed by concrete crushing. For beams B8-2/S-10 and B9-2/L-10, compressive strain at the top of the beam was greater than 0.004.

DIC strains were obtained dividing the relative displacement between two points located the same vertical position by their distance (approximately 200 mm). In general, good agreement was achieved between strain gage readings and those obtained using DIC, validating the image correlation analysis. Moment-curvature relationships obtained using DIC are presented in Figure 4a. It can be seen that all beams reached curvatures greater than 0.1 m^{-1} . For the cross-section studied, this value corresponds approximately to a steel strain of 0.01 and concrete strain close to 0.003, which is acceptable in terms of required ductility. RC beams exhibited gain of capacity after yielding, which is associated to the strain hardening behavior of reinforcing steel. On the other hand, peak moments for R/SFRC beams occurred for a curvature coinciding with the beginning of yielding of steel rebars, Φ_y , followed by a gradual reduction of moment with increasing curvature, which is associated to the tensile stress decay. In Figure 4b, load-deflection curves are also presented, showing a similar behavior and confirmed that use of fibers resulted in loss of ductility.



Figure 3: Failure modes observed for RC and R/SFRC beams: a) B3-0-10; b) B9-2/L-10.



(a)

(b)

Figure 4: Beams response: a) moment-curvature; and b) load-deflection.

A summary of the main results obtained from moment-curvature relationships is presented in Table 4. Significantly increase in the moment at yielding, M_y , was achieved with the use of fibers, with ratios between R/SFRC and RC beams ($M_{R/SFRC}/M_{RC}$) ranging from 1.21 to 2.09. Increases in cracked stiffness, $(EI)_{\text{cracked}}$, were also obtained with increasing fiber content. Finally, moment capacities for a curvature of 0.1 m^{-1} , $M_{0.1}$, were compared to those computed with Henager and Doherty's approach, M_{HD} , leading to a good agreement, especially for beams containing 10-mm diameter rebars. Differences with respect to other rebars may be explained by deviations in mechanical properties of rebars used.

Table 4: Summary of results for beam tests.

Specimen	M_y (kN.m)	$M_{0.1}$ (kN.m)	Φ_y (m^{-1})	$(EI)_{\text{cracked}}$ (kN.m ²)	$M_{R/SFRC}/M_{RC}$	$M_{0.1}/M_{HD}$
B1-0-6	4.84	4.97	0.045	108	-	0.86
B2-0-8	7.05	7.82	0.039 ^(SG)	181	-	0.77
B3-0-10	9.60	10.4	0.036	267	-	1.01
B4-0.5/S-10	11.6	11.5	0.046	252	1.21	1.01
B5-1/S-10	13.2	12.5	0.039	338	1.38	0.97
B6-2/S-6	10.1	8.73	0.037	273	2.09	0.76
B7-2/S-8	11.2	10.2	0.043	260	1.59	0.85
B8-2/S-10	14.2	*	0.032 ^(SG)	444	1.48	*
B9-2/L-10	15.0	14.9	0.031	484	1.56	0.97

^(SG) data obtained using strain gage

* malfunction

With the constitutive relationships for the materials, it is also possible to develop non-linear cross-section analysis to obtain a full theoretical moment-curvature relationship. A comparison between predicted and experimental moment-curvature for beams B3-0-10, B5-1/S-10 and B9-2/L-10 are presented in Figures 5a, 5b and 5c, respectively. Excellent agreement was achieved between models and experiments and the contributions of reinforcing steel and concrete in tension to the bending capacity can be obtained from the model.

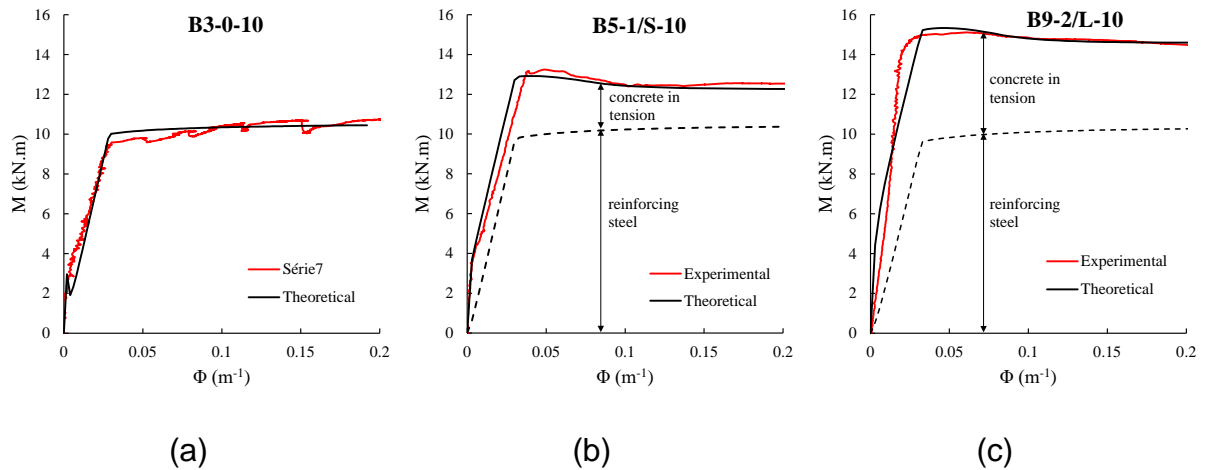


Figure 5: Comparison between theory and experiment and contributions of fiber in tension and reinforcing steel: a) B3-0-10; b) B5-1/S-10; c) B9-2/L-10.

Regarding crack formation and growth, a comparison between beams B2-0-8 and B7-2/S-8 is presented in Figure 6. It can be seen that cracks for R/SFRC beams are thinner even for greater bending moments. For example, crack openings smaller than 0.3 mm were obtained for a bending moment $M = 11.1$ kN.m applied to B8, whereas openings close to 0.9 mm were measured for $M = 7.3$ kN.m applied to B2. In general, a critical section with a wider crack clearly distinguishable from the others could be identified. This is likely associated with a lesser fiber content in that section, leading to a considerable fiber pullout when compared to other sections. This may also explain the fact that, in some cases, cracks other than the critical cannot be seen with naked eye. However, as shown in Figure 6, these ‘invisible’ cracks can be captured using DIC.

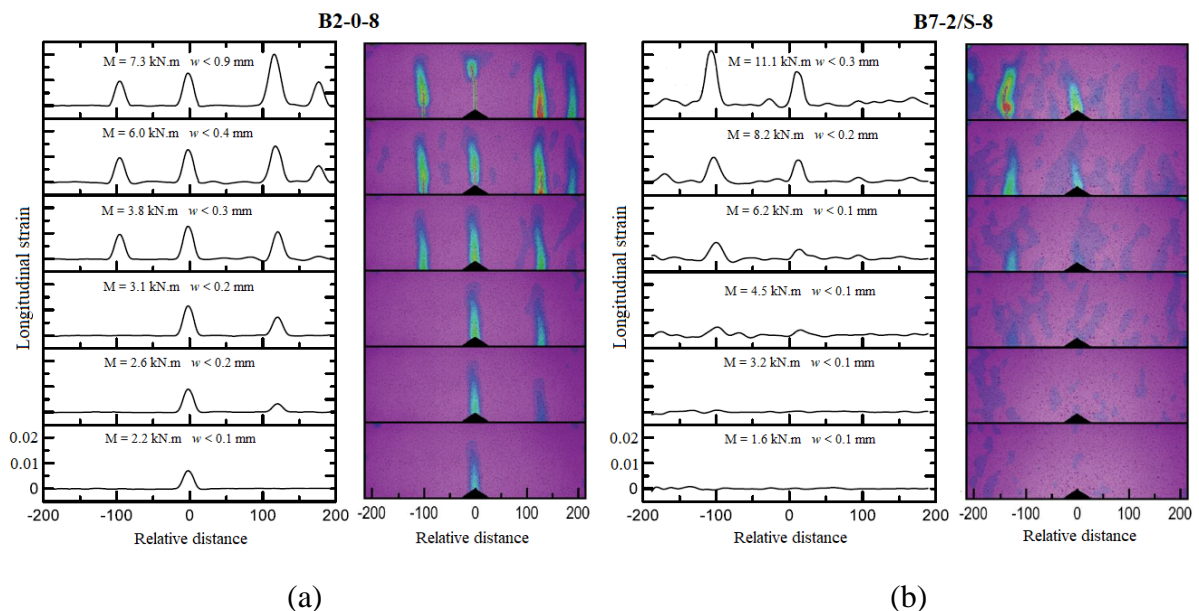


Figure 6: Crack pattern and growth: a) B2-0-8; b) B7-2/S-8.

4. CONCLUSIONS

In this work, behavior of R/SFRC beams subject to flexure was studied. Full material characterization was carried out and under-reinforced beams having different fiber contents

and reinforcing ratios were tested under 4-point bending and monitored using DIC. The following conclusions can be drawn from the study:

- DIC proved to be suitable non-contact method to monitor curvature and crack formation and growth in reinforced concrete structures;
- Increases in moment capacity ranging from 21 to 109% were achieved with the use of fiber reinforced concrete matrix with respect to plain concrete. Cracked stiffness was also improved with increasing fiber contents;
- Theoretical predictions with cross-section analysis using actual non-linear constitutive relationships proved to be useful to predict behavior and can be extended to other cross-section configurations and material properties;
- Thinner cracks were obtained for R/SFRC beams even for greater loads. Crack pattern of R/SFRC crack was also different from RC, characterized by a critical wider crack and multiple thin cracks, sometime imperceptible.

ACKNOWLEDGMENTS

The authors acknowledge Brazilian research agencies (CAPES, CNPq and FAPERJ) for financial support and Lafarge-Holcim and Ibrata for supplying the material for the research. Authors would like to express their gratitude to Dr. Giancarlo Gonzáles and Prof. José Roberto Freire for the valuable support with DIC analysis.

REFERENCES

- [1] Di Prisco, M., Plizzari, G., & Vandewalle, L. (2009). Fibre reinforced concrete: new design perspectives. *Materials and Structures*, 42(9), 1261-1281.
- [2] Sorelli, L. G., Meda, A., & Plizzari, G. A. (2006). Steel fiber concrete slabs on ground: a structural matter. *ACI Structural Journal*, 103(4), 551.
- [3] Chiaia, B., Fantilli, A. P., & Vallini, P. (2009). Combining fiber-reinforced concrete with traditional reinforcement in tunnel linings. *Engineering Structures*, 31(7), 1600-1606.
- [4] Carter W. (1971). Wire-reinforced precast concrete decking panels, *Precast Concrete (UK)*, pp. 703-708.
- [5] Dinh, H. H., Parra-Montesinos, G. J., & Wight, J. K. (2010). Shear strength model for steel fiber reinforced concrete beams without stirrup reinforcement. *Journal of Structural Engineering*, 137(10), 1039-1051.
- [6] Henager, C. H., & Doherty, T. J. (1976). Analysis of reinforced fibrous concrete beams. *Journal of the Structural Division*, 102.
- [7] Swamy, R. N., and Al-Ta'an, S. A. (1981). Deformation and ultimate strength in flexure of reinforced concrete beams made with steel fiber concrete. *ACI Journal*, 395-405.
- [8] Oh, B. H. (1992). Flexural analysis of reinforced concrete beams containing steel fibers. *Journal of Structural Engineering*, 118(10), 2821-2835.
- [9] Bentur, A., & Mindess, S. (1983). Concrete beams reinforced with conventional steel bars and steel fibres: properties in static loading. *International Journal of Cement Composites and Lightweight Concrete*, 5(3), 199-202.
- [10] Abdul-Ahad, R. B., & Aziz, O. Q. (1999). Flexural strength of reinforced concrete T-beams with steel fibers. *Cement and Concrete Composites*, 21(4), 263-268.
- [11] Fib, Fédération Internationale du Béton (2010). fib model code for concrete structures 2010, October 2013. Berlin: Ernst&Sohn.
- [12] van Zijl, G. P. A. G., & Mbewe, P. B. K. (2013). Flexural modelling of steel fibre-reinforced concrete beams with and without steel bars. *Engineering Structures*, 53, 52-62.
- [13] Mertol, H. C., Baran, E., & Bello, H. J. (2015). Flexural behavior of lightly and heavily reinforced steel fiber concrete beams. *Construction and Building Materials*, 98, 185-193.
- [14] Lim, T. Y., Paramasivam, P., & Lee, S. L. (1987). Behavior of reinforced steel-fiber-concrete beams in flexure. *Journal of Structural Engineering*, 113(12), 2439-2458.

- [15] Mobasher, B., Yao, Y., & Soranakom, C. (2015). Analytical solutions for flexural design of hybrid steel fiber reinforced concrete beams. *Engineering Structures*, 100, 164-177.